2-D wavelength demultiplexer with potential for ≥ 1000 channels in the C-band

Shijun Xiao and Andrew M. Weiner

School of Electrical & Computer Engineering, Purdue University, West Lafayette, IN 47907-1285, U.S.A.
sxiao@ecn.purdue.edu, amw@ecn.purdue.edu

Abstract: We demonstrate a 2-D wavelength demultiplexer by using a virtually imaged phased array (VIPA) and a diffraction grating in bulk optics, which yields a hyperfine channel spacing 5 GHz (40 pm) with 1.75 GHz (14 pm) -3dB bandwidth, >20dB channel isolations, and a very large free spectral range. The 2-D wavelength demultiplexer is capable of having a very large number (≥1000) of hyperfine channels in the C-band (1530 - 1570 nm). We also present the first analytic theory for the 2-D demultiplexer.

©2004 Optical Society of America

OCIS codes: (060.2330) Fiber optics communications, (060.1810) Couplers, switches, and multiplexers

---

References and Links

1. K. Takada, M. Abe, T. Shibata, K. Okamoto, "10-GHz-spaced 1010-channel tandem AWG filter consisting of one primary and ten secondary AWGs," IEEE Photon. Technol. Lett. **13**, 577-578 (2001).
2. M. Shirasaki, "Large angular dispersion by a virtually imaged phased array and its application to a wavelength demultiplexer," Opt. Lett. **21,** 366-368 (1996).
3. S. Xiao, A. M. Weiner, C. Lin, "Demultiplexers with ~ 10 pm (1.25 GHz) -3dB transmission bandwidth using a virtually imaged phased array (VIPA)," TuL1, Optical Fiber Communication Conference, (Optical Society of America, Washington D.C., 2004).
4. S. Xiao, A. M. Weiner, C. Lin, "Experimental and theoretical study of Hyperfine WDM Demultiplexer performance using the virtually-imaged phased-array (VIPA)," submitted to IEEE/OSA J. Lightwave Technol.
5. S. Xiao, J. D. McKinney, A. M. Weiner, "Photonic microwave arbitrary waveform generation using a virtually-imaged phased-array (VIPA) direct space-to-time pulse shaper," in press, IEEE Photon. Technol. Lett. (2004).
6. A. M. Weiner, "Femtosecond pulse shaping using spatial light modulators," Rev. Sci. Instrum. **71**, 1929-1960 (2000).
7. R. D. Nelson, D. E. Leaird, A. M. Weiner, "Programmable polarization-independent spectral phase compensation and pulse shaping," Opt. Express, **11**, 1763-1769 (2003).
8. M. Shirasaki, "Compensation of chromatic dispersion and dispersion slope using a virtually imaged phased array", TuS1, Optical Fiber Communication Conference, (Optical Society of America, Washington D.C., 2001).
9. S. Xiao, A. M. Weiner, C. Lin, "A dispersion law for virtually-imaged phased-array (VIPA) spectral dispersers based on paraxial wave theory," IEEE J. Quantum Electron. **40**, 420- 426 (2004).

---

1. Introduction

Technology for separating and combining wavelengths is fundamental to wavelength division multiplexing (WDM). Multiplexing-demultiplexing devices with substantially narrower linewidth could lead to new opportunities for networks with finer wavelength granularity and larger channel counts, as well as new possibilities for optical signal processing. With the well-known arrayed waveguide grating (AWG) technology, channel spacing is limited to 10 GHz, with -3dB bandwidth limited to 4 GHz. An experiment using one primary AWG and 10 secondary AWGs operating at this channel spacing demonstrated demultiplexing of 500 channels within the C-band (1530 nm -1570 nm) [1]. Using a relatively new optical demultiplexer termed a virtually-imaged phased-array (VIPA) [2], we have recently shown

very narrow demultiplexing linewidths, with -3dB bandwidths of 1 and 2 GHz (8 and 16 pm) for 50 and 100 GHz free spectral range (FSR) devices, respectively [3, 4]. This narrow linewidth capability makes the VIPA attractive for applications in hyperfine WDM and in femtosecond pulse shaping with unusually large time apertures (~1 ns) [5]. For the VIPA demultiplexer, the narrow -3dB bandwidths are linked to a periodic spectral dispersion behavior with relatively low FSR; this strongly limits the channel counts available for wavelength division multiplexing applications. Recently, a combination of a VIPA and a diffraction grating has been used in a Fourier pulse shaping geometry [6, 7] to implement a chromatic dispersion compensation system with varied dispersion slope for different WDM channels [8], where the VIPA separates wavelength components within a single WDM channel in one dimension, and the diffraction grating separates different WDM channels into another dimension. Here, for the first time to our knowledge, we investigate the 2-D wavelength demultiplexing performance of this approach. We demonstrate 1.75 GHz -3dB linewidth while essentially fully suppressing the free-spectral-range behavior. Our measurements demonstrate 41 channel demultiplexing with 5 GHz channel spacing in a 1.6 nm wavelength band with channel isolation > 20 dB. Our results should scale to $\geq$ 1000 channels in the C-band in a single 2-D wavelength demultiplexer apparatus.

The VIPA is a relatively new optical spectral disperser based on a "side-entrance" Fabry-Perot etalon geometry. It typically consists of two glass plates, of which the back or the transmission side is coated with a partially reflective film (e.g., r $\geq$ 95%); the front or entry side is coated with an almost R~100% reflective film except in a window area, which is uncoated or antireflection (AR) coated. If the etalon cavity is filled with air, it is called an air-spaced VIPA; otherwise if it is filled with some glass of refractive index n_r, it is called a solid VIPA. A collimated beam is focused by a cylindrical lens into the VIPA at a small angle through the window area, and the injected beam experiences multiple reflections between two plates of the VIPA. The angular dispersion is achieved via multiple beam interference. An important property of the VIPA is that it can provide over an order of magnitude larger angular dispersion than typical diffraction gratings [2, 9].

2. Setup

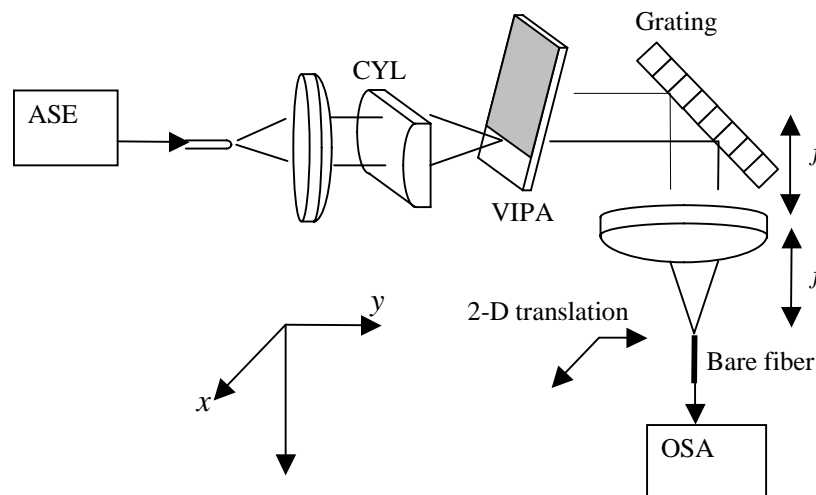

Fig. 1. The layout of our 2-D spectral disperser. The grating disperses in y; the VIPA disperses in x. OSA: optical spectrum analyzer with 0.01 nm resolution in wavelength. CYL: cylindrical lens.

Figure 1 shows our experimental setup. A solid VIPA with some glass of a refractive index n_r~2 and a thickness t~1.5mm (FSR ~ 50 GHz) is used. The diffraction grating has a groove

density of 1100 lines/mm. The amplified spontaneous emission (ASE) source has a flat band ~ 30 nm centered at 1.55 um. A collimated beam (intensity falls to $1/e^2$ at radius W=1.2 mm compared to the center) from the source is focused into the VIPA by a cylindrical lens with focal length f_c in the x dimension, and then the VIPA output (still collimated in y dimension) is diffracted by the diffraction grating in y dimension. The beam incident angle θ_i into the VIPA is ~ 4°, and the beam incident angle on the grating is θ_{ig} ~ 70° with a diffracted angle θ_d ~ 50°. A spherical lens (f =180 mm) focuses all beams onto the back focal plane, where a bare single mode fiber (9/125 um) connected to an optical spectrum analyzer (OSA) samples the transmission spectra. The OSA has a spectral resolution of 0.01nm. The 2-D demultiplexing can be understood in the following way. First, assuming no diffraction grating in the setup, the VIPA maps multiple peak wavelengths (multiple transmission peaks) with 50 GHz (0.4nm) period onto the same x position. If a diffraction grating is now used to disperse optical wavelengths in the y dimension, the multiple peak wavelengths with 50 GHz FSR separation at a single x position will now separate to different y positions. Figure 2 shows a photograph of our 2-D wavelength demultiplexer. (Note that the beam expander shown in the photo is used only for our later experiment in connection with the data of Fig. 5.)

We note that VIPAs are expected to have very low polarization dependent loss (PDL) [2]. In principle, a low PDL grating can also be used in our setup, which means that a 2-D spectral disperser with low PDL is possible. In the present experiments, we do not use a low PDL grating, and therefore the 2-D spectral disperser works preferentially with y-polarized light.
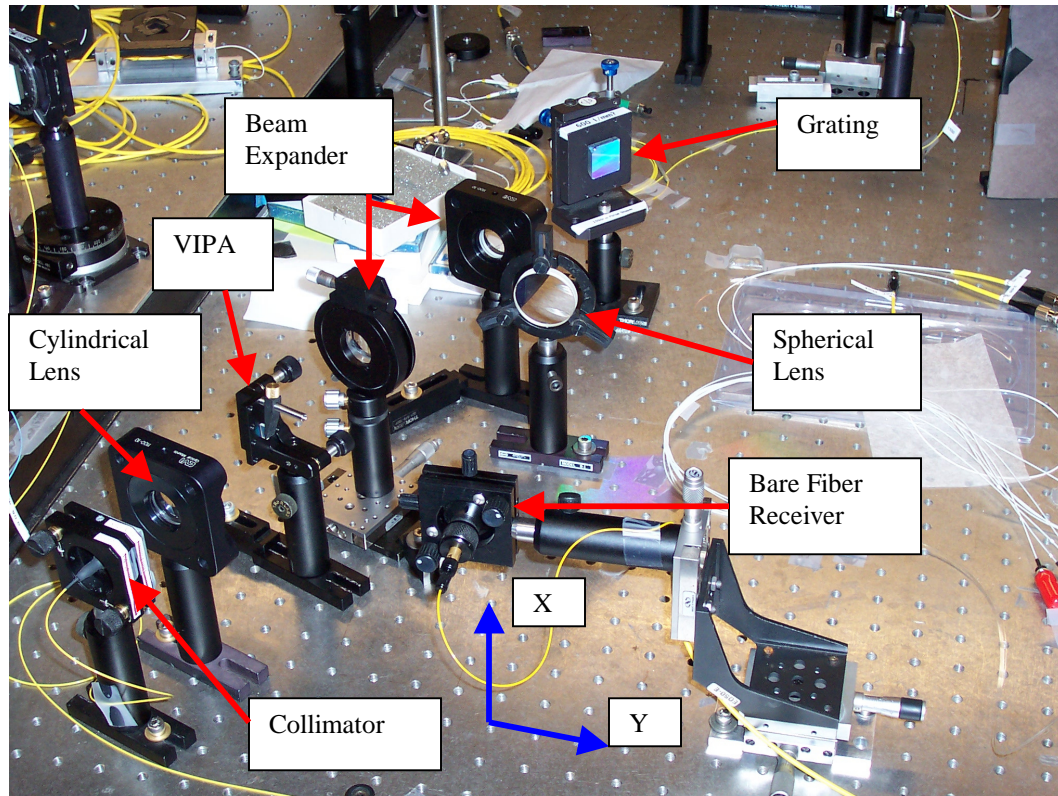

Fig. 2. Photograph of our 2-D wavelength demultiplexer. (The beam expander shown in the photo is used only for our later experiment in connection with the data of Fig. 5.)

3. Theory

Assuming dispersion in x and dispersion in y are independent, the intensity distribution dependence in space and wavelength is just the product of the distribution from the VIPA [9] and the distribution from the grating [6]

$$I_{out}(x, y, \lambda) \propto I_{in}(\tilde{\omega}) \exp\left(-2\frac{f_c^2 x^2}{f^2 W^2}\right) \frac{1}{(1-Rr)^2 + 4(Rr)\sin^2\left(\frac{k\Delta}{2}\right)} \exp\left[-\frac{(y-\alpha\tilde{\omega})^2}{w_0^2}\right]$$

(1)

where, $w_0 = \dfrac{\cos(\theta_{ig})}{\cos(\theta_d)}\dfrac{f\lambda}{\pi W}$ is the focused beam waist in y, $\alpha = \dfrac{\lambda^2 f}{2\pi c d \cos(\theta_d)}$ is the grating dispersion

parameter, $\Delta = 2t\,n_r\cos(\theta_{in}) - 2t\dfrac{\tan(\theta_{in})\cos(\theta_i)x}{f} - t\dfrac{\cos(\theta_{in})x^2}{n_r f^2}$ is the VIPA

dispersion parameter, $I_{in}(\tilde{\omega})$ is the input spectrum, $\tilde{\omega} = \omega - \omega_o$ is the offset from the center

frequency, and $k = \dfrac{\omega}{c} = \dfrac{2\pi}{\lambda}$ is the wave vector.

Equation (1) is the master equation that predicts the wavelength demultiplexing characteristics in both space and spectrum dimensions as well as the demultiplexing linewidth.

The spatial dispersion of the VIPA disperser is [9]

$$\lambda_p - \lambda_0 = -\lambda_0\left[\frac{\tan(\theta_{in})\cos(\theta_i)}{n_r\cos(\theta_{in})}\frac{x}{f} + \frac{1}{2}\frac{1}{n_r^2}\frac{x^2}{f^2}\right]$$

(2)

where, $m\lambda_0 = 2tn_r\cos(\theta_{in})$, $\theta_{in} = \theta_i/n_r$ is the beam angle inside the VIPA, and $\lambda_p(x)$ is a wavelength whose intensity distribution peaks at position x.

The grating spatial dispersion is

$$\lambda_p - \lambda_0 = d\cos(\theta_{d_0})\frac{y-y_0}{f}$$

(3)

where, $d\sin(\theta_{d_0}) + d\sin(\theta_{ig}) = \lambda_0$, and y_0 is the spatial position of peak wavelength λ_0.

As the grating filter has a -3dB bandwidth of tens of GHz, which is an order of magnitude larger than that of the VIPA filter, the -3dB bandwidth is mainly determined by the VIPA demultiplexer according to master Eq. (1):

$$FWHM/_{frequency} = \frac{c}{2\pi t\,n_r\cos(\theta_i)}\frac{1-Rr}{\sqrt{Rr}},$$

$$FWHM/_{wavelength} = \frac{\lambda_0^2}{2\pi t\,n_r\cos(\theta_i)}\frac{1-Rr}{\sqrt{Rr}}$$
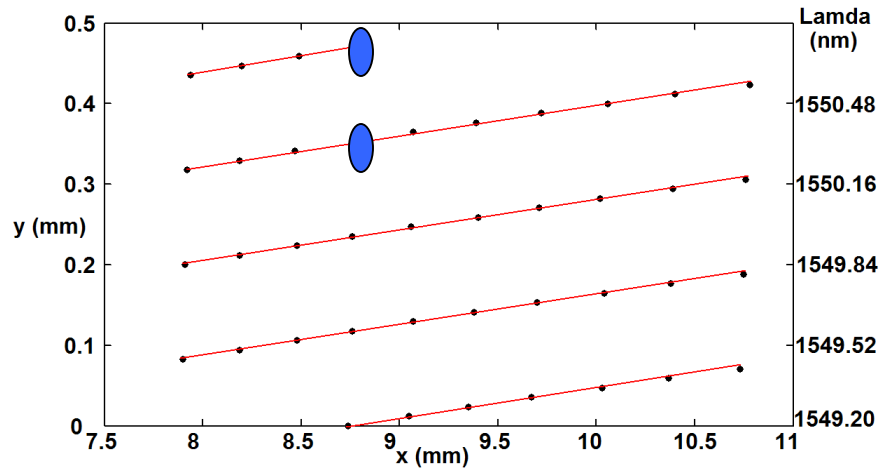
(4)

4. Experiments

Fig 3. The 2-D wavelength demultiplexing. Peak wavelengths are demultiplexed to different (x, y). The red solid lines are approximate linear fittings to the demultiplexing data. The blue ellipses show the size at half maximum of the peak intensity for two selected peak wavelengths.

For the 2-D demultiplexing, it is interesting to display the peak wavelengths corresponding to various 2-D positions (x, y). In our testing, we look at 41 peak wavelengths ranging from 1549.20 nm to 1550.80nm with a step of 0.04 nm (5GHz). Figure 3 shows the (x, y) corresponding to all these chosen peak wavelengths. The x and y are readings from the micrometer with 0.01 mm resolution. The red solid lines in the plot are approximate linear fittings for the wavelength dispersion data, and it results from multiple diffraction orders of the VIPA. The beam incident angle θ_i into the VIPA is $4.2^o \pm 0.2^o$, which results in an approximate linear dispersion dominated by the first term on the right side in the Eq. (2). The blue ellipses in Fig. 3 show qualitatively the spatial intensity distribution of two specific wavelengths, where the boundary indicates positions with half maxima compared to the peak. The key point is that adjacent different orders of the VIPA are clearly separated in space. Experiments show 80 ± 10 um and 50 ± 10 um in diameter for the ellipse in both x and y direction, which agree well with our theory.
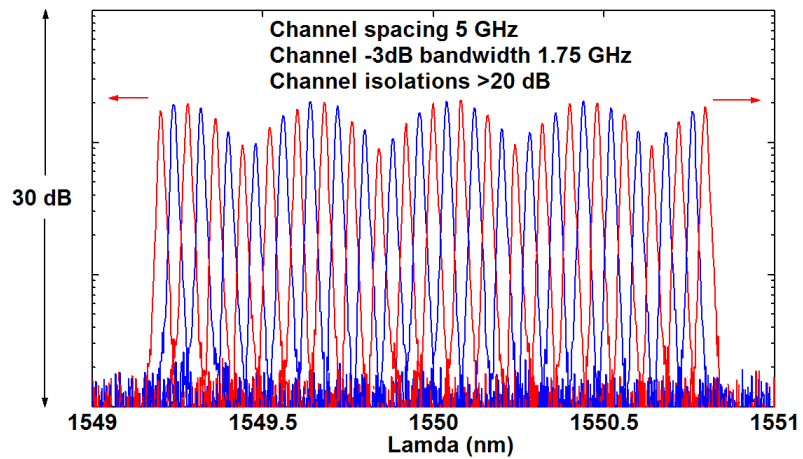
(a)
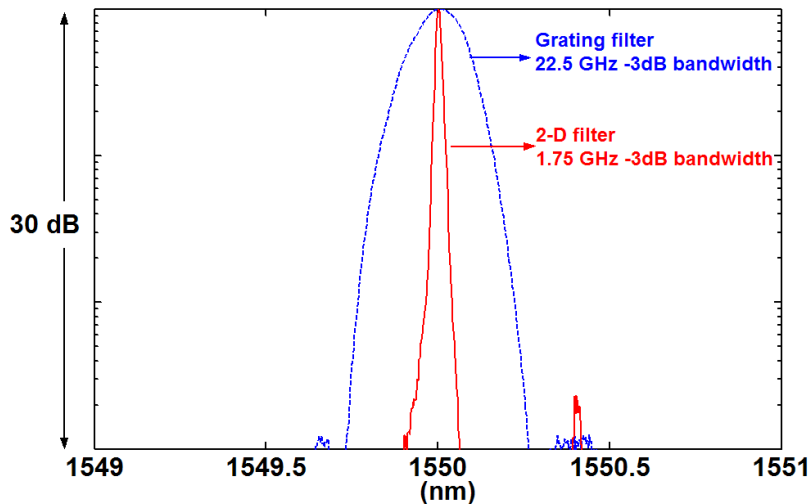
(b)

Fig. 4. (a) is the 2-D multiple demultiplexing channels with center channel wavelengths corresponding to the data in Fig. 3, and (b) is the corresponding channel lineshape.

Figure 4(a) shows the lineshapes of the 41 2-D demultiplexing channels, corresponding to the spatial positions in Fig. 3. Experimentally, we show a channel spacing 5GHz (0.04 nm), a channel -3dB bandwidth of 1.75 GHz and good channel isolations > 20dB. The periodic intensity modulation at the VIPA's FSR (0.4 nm) results from transitions between dominant VIPA diffraction orders together with the Gaussian roll-off of the envelope as a function of x, which is fully modeled by our master equation (1). Note that the 1.6 nm band tested in Fig. 4(a) was chosen solely for experimental convenience. In principle, our scheme should extend equally over a very wide band. Thus, we demonstrate a new scheme with potential for ≥ 1000 hyperfine channels using the 2-D demultiplexer based on the VIPA and the diffraction grating in bulk optics.

Figure 4(b) shows the normalized lineshape for one of those channels in greater detail. The blue dashed one is the grating filter's Gaussian lineshape without inserting the VIPA, and the red solid curve is the lineshape of the 2-D demultiplexer. The right side lobe on the 2-D demultiplexer's lineshape is a small residue arising from the 50 GHz FSR of the VIPA; the side lobe is suppressed down to -25 dB compared to the peak level of the grating filter alone. The lack of complete suppression is attributed to the fact that the limited aperture of our VIPA in the y direction slightly clips the input beam to the grating, which slightly distorts the grating filter lineshape. The observed -3dB bandwith of 1.75 GHz (14 pm) is largely determined by the VIPA filter. In addition, by taking into account the finite spectral resolution of the OSA (10 pm), we estimate that the actual lineshape has ~ 1.25 GHz (10 pm) -3dB bandwidth [3, 4], which allows a smaller channel spacing.
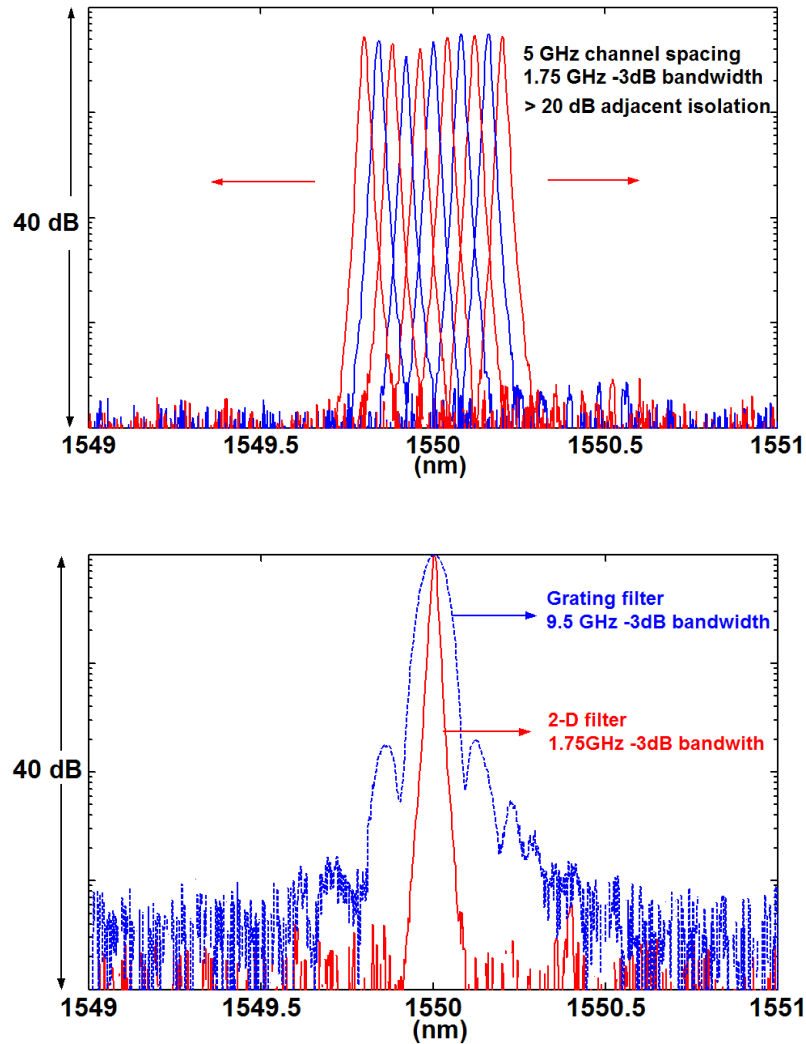

Fig. 5. (a) is another sample of the demultiplexing channel response with improved insertion loss performance and same spatial dispersion compared to Fig. 4, and (b) is the corresponding channel lineshape.

For practical 2-D hyperfine WDM systems, the insertion loss for the peak wavelength is also an important performance parameter. In our experiments above, the insertion loss for the 2-D demultipexer is not optimized due to the relatively large focusing spot size (~ 80 um in x and ~ 50 um in y). In addition, it is desirable to further suppress the residual side lobes due to the VIPA's FSR (Fig. 4(b)) for even lower channel crosstalk. A feasible way to optimize both the insertion loss performance and side lobe suppression is to use collimated beams with larger radius W, which would result in smaller focused spot size in y for the grating and also narrower bandwidth for the grating filter. Currently, we are limited by the VIPA aperture size in y. Instead of using a collimator with larger beam radius, it is possible to do this with a beam expander in y only between the VIPA and the grating. Therefore, in another experiment, we inserted a beam expander (4×) working in y based on two cylindrical lenses between the VIPA and the grating (Fig. 2.). All other experimental conditions were left unchanged. The channel response is maintained while the side lobes are suppressed to lower than 30dB down compared to the peak level (Fig. 5). The 2-D dispersion relationship is the same as in Fig. 3; the beam expander doesn't change the dispersion relation. For simplicity, we have plotted only a group of 11 channels in a 0.4 nm range in Fig. 5(a); however, as indicated in Fig. 4(a), it is possible to extend over the entire C-band. The total insertion loss is ~ 17 dB for y-polarized light, and the total insertion loss is 4 - 5 dB less than the first setup. Lower insertion loss should be possible using a beam expander with larger expanding factor for close mode-matched coupling into the single mode fiber. The ripples on the wings of the grating filter lineshape are due to small beam clippings both at the grating edge and at the VIPA in y according to our experiments. In principle, the insertion loss performance could be optimized further by tighter focusing in x. One approach for achieving this would be to incorporate independent cylindrical focusing in x and y between the grating and the receiving fiber. In principle, we may have a very low insertion loss assuming we obtain mode-matched coupling in both x and y for the single mode fiber receiver while maintaining the channel response.

5. Conclusion

In summary, we demonstrate a 2-D wavelength demultiplexer with a narrow -3dB bandwidth of 1.75 GHz determined by the VIPA filter and a very large FSR determined by the diffraction grating. We present a simple analytic theory for the 2-D wavelength demultiplexer. Experimentally, we show demultiplexing channels with a spacing of 5 GHz and good channel isolations > 20dB, which has the potential to allow hyperfine WDM with channel number $\geq$ 1000 in the C-band. We also show the possibility of increasing the side lobe suppression to > 30 dB. In future work, we are interested in investigating 2-D waveguide-fiber arrays for output coupling as well as reflective Fourier transform pulse shaping [6, 7] using the 2-D wavelength demultiplexer, where it may be easier to realize low insertion loss.